Talanta 101 (2012) 24–31

Contents lists available at SciVerse ScienceDirect

Talanta

journal homepage: www.elsevier.com/locate/talanta

Improvement of sensitive CuO NFs–ITO nonenzymatic glucose sensor based on in situ electrospun fiber

Guangyue Liu [a], Baozhan Zheng [a], Yanshu Jiang [a], Yuqing Cai [a], Juan Du [a], Hongyan Yuan [b], Dan Xiao [a,b,*]

[a] College of Chemistry, Sichuan University, No. 29 Wangjiang Road, Chengdu 610064, PR China
[b] College of Chemical Engineering, Sichuan University, No. 29 Wangjiang Road, Chengdu 610065, PR China

ARTICLE INFO

Article history:
Received 5 June 2012
Received in revised form
16 August 2012
Accepted 27 August 2012
Available online 4 September 2012

Keywords:
Non-enzymatic glucose sensors
Electrospun nanofibers
Copper oxide

ABSTRACT

CuO nanofibers (NFs), prepared by electrospinning and calcination technologies, have been applied for the fabrication of glucose sensors with high sensitivity and selectivity. $Cu(NO_3)_2$ and polyvinylpyrrolidone (PVP) composite nanofibers were initially electrospun on the surface of indium tin oxide (ITO) glass, and then the CuO NFs–ITO electrode was formed simply by removing PVP through heat treatment. The structures and morphologies of CuO nanofibers were characterized by X-ray diffraction, scanning electron microscopy and thermogravimetric analysis. The direct electrocatalytic oxidation of glucose in alkaline medium at CuO NFs–ITO electrode has also been investigated in detail with cyclic voltammetry, chronoamperometry and electrochemical impedance spectroscopy. The effects of NaOH concentration, electrospinning time, $Cu(NO_3)_2$:PVP mass ratios and calcination temperature on the response to glucose were investigated. Under optimized experimental conditions, the CuO NFs–ITO electrode produced high and reproducible sensitivity to glucose of $873\ \mu A\ mM^{-1}\ cm^{-2}$. Linear responses were obtained over a concentration range from 0.20 μM to 1.3 mM with a detection limit of 40 nM ($S/N=3$). The CuO NFs–ITO electrode also has good selectivity, stability and fast amperometric sensing of glucose, thus it can be used for the future development of non-enzymatic glucose sensors.

1. Introduction

The maintenance of glucose level in human or animal blood is very important and any deviance from the normal glucose level may induce sickness and disease. Therefore, the development of highly sensitive and selective glucose sensors has attracted much attention due to its importance in areas of biotechnology, clinical diagnostics and the food industry [1–3]. As known, glucose sensors can be mainly classified into two categories: glucose oxidase (GOD) based sensing and non-enzymatic glucose sensing. Due to the high sensitivity and selectivity to glucose, GOD has been widely used to construct various amperometric biosensors for glucose detection [4–7]. However, the greatest drawback of GOD-based sensors is that the insufficient stability, which originated from the intrinsic nature of the enzyme to both pH and temperature, can hardly be overcome. Therefore, more and more attempts have been made to construct sensors for the glucose detection without the use of enzymes. The majority of these nonenzymatic electrochemical glucose sensors rely on the current response of glucose oxidation directly at the electrode surface. In order to improve the sensitivity and selectivity of the sensor, various nanostructured metals (Pt, Au, Pd, Ni, Cu) [8–12], alloys (Pt–Pb, Pt–Au, Au–Ru) [13–15] and metal oxides (Co_3O_4, NiO, CuO) [16–18] have been explored as the working electrode materials for the direct electro-catalyzing oxidation of glucose.

Copper oxide (CuO), a p-type semiconductor with a narrow band gap of 1.2 eV, has been studied intensely because of its numerous applications in catalysis, semiconductors, batteries, gas sensors, biosensors, and field transistors [19–24]. With the development of nanotechnology, nanostructured CuO is promising in the development of nonenzymatic glucose sensors because of its highly specific surface area, good electrochemical activity, and the possibility of promoting electron transfer reactions at a lower overpotential [25]. The shapes and dimensions of the nanomaterials have a great influence on their properties [26,27]. Therefore, many kinds of nanostructured CuO have been produced such as nanowires [16], nanospheres [25], nanoflowers [27], and nanorods [27], and these nanostructures can enhance their intrinsic characteristics and performances on amperometric determination of glucose. However, most of these nanostructures fabrications are complicated and time-consuming. Therefore, there still remains a need for simpler processes to synthesize novel CuO nanostructures with superior catalytic property for fast, sensitive, and stable detection of glucose.

Nowadays, electrospinning technology has attracted significantly increasing attention as a versatile and cost-effective

---

[*] Corresponding author at: College of Chemistry, Sichuan University, No. 29 Wangjing Road, Chengdu, Sichuan 610064, China. Tel.: +86 28 85416029; fax: +86 28 85415029.
E-mail address: xiaodan@scu.edu.cn (D. Xiao).

0039-9140/$ - see front matter © 2012 Elsevier B.V. All rights reserved.
http://dx.doi.org/10.1016/j.talanta.2012.08.040

method for producing long continuous fibers with diameters ranging from several micrometers down to a few nanometers [28,29]. The remarkable specific surface area, high porosity and good structural controllability make electrospun nanomaterials highly attractive to ultrasensitive sensors and of increasing importance in other nanotechnological applications [30,31]. Until now, great efforts have been made to fabricate different electrospun nanofibers for nonenzymatic glucose sensors. Due to their high surface-to-volume ratios and low cross-section areas, the elctrospun nanofibers could lead to more effective performances of electrochemical detectors, such as in mass transport, the electric charge transport and the signal to noise current ratios [31]. With the great development of nanotechnology, various electrospun nanomaterials such as Ni nanoparticle-loaded carbon nanofibers [32], copper oxide nanofibers [33], cobalt oxide nanofibers [17] and nickel oxide microfibers [34] were explored as the candidates in the hope of developing effective enzyme-free glucose sensors.

Copper oxide nanofibers prepared by electrospinning and subsequent calcination processes have been used to construct nonenzymatic sensor for the detection of glucose by Wang et al. [33]. The sensor has a high sensitivity to glucose and a long-term stability. However, in the process of electrode preparation, CuO nanofibers were dispersed firstly into suitable solvents by ultrasonication, and then the suspension was cast onto the electrode surface to immobilize CuO nanofibers. This process was not only time-consuming, but also the sonication process may affect the morphology of 1-D CuO nanofibers and affect the catalytic activity to glucose finally.

In this work, precursor nanofibers with $Cu(NO_3)_2$ dissolved in poly(vinyl pyrrolidone) (PVP) were directly electrospun onto indium tin oxide (ITO) surfaces. It was then calcinated in air to remove the matrix polymer of PVP and convert the precursor fibers into CuO nanofibers. This process of electrode preparation is simple and convenient, more importantly, the direct preparation of CuO nanofiber on ITO ensures fast electron transfer between the CuO nanofibers and the ITO electrode, which could enhance the sensitivity of sensor to glucose. The CuO nanofibers on the ITO surface are very stable and have a fast response to glucose, so it could be used directly as the working electrode to detect glucose. In order to obtain a higher sensitive sensor, some preparation and measurement conditions, such as the NaOH concentration, electrospinning time, the $Cu(NO_3)_2$:PVP mass ratios, and calcination temperature, were investigated by means of chronoamperometry. Under the optimized experimental conditions, the CuO NFs–ITO electrode presents better sensitivity and stability, a low detection limit and fast amperometric response. In addition, our proposed sensor also offers better selectivity, long-term stability, and immunity to chloride poisoning. It is anticipated that our CuO nanofibers could be promising for the development of non-enzymatic glucose sensors.

2. Experiment

2.1. Reagents

Polyvinylpyrrolidone (PVP, $Mw=1{,}300{,}000$) and uric acid (UA) were purchased from Acros (New Jersey, USA). Dopamine hydrochloride (DA) was obtained from Alfa Aesar (Johnson Matthey Company, Tianjin, China). Glucose ($C_6H_{12}O_6 \cdot H_2O$), sodium hydroxide (NaOH), sodium chloride (NaCl), ascorbic acid (AA) and sucrose were obtained from Chengdu Kelong Chemical Company (Chengdu, China). Copper nitrate ($Cu(NO_3)_2 \cdot 3H_2O$) was from Tianjin Jingxin Chemical Reagent Factory (Tianjin, China). Ethanol (C_2H_5OH) was purchased from Tianjin Meilin Industry & Trade Co., Ltd. (Tianjin, China). Lactose was from Guangdong Xilong Chemical Company (Shantou, China), and soluble starch was from Chengdu Hongbo Industry Co., Ltd. (Chengdu, China). All chemicals were of analytical grade and used as received. All solutions were freshly prepared with doubly distilled water (DDW).

2.2. Preparation of CuO NFs–ITO film electrodes.

Like the typical procedure for preparing metal oxide nanofibers through electrospinning [35,36], CuO nanofibers were fabricated by three steps: I) For the preparation of precursor solution, 0.30 g PVP as the matrix polymer was dissolved in 2.0 mL absolute ethanol, and stirred for 12 h to form homogeneous solutions. Then, 1 mL 0.15 g mL^{-1} $Cu(NO_3)_2$ aqueous solution was added into PVP ethanol solution, and the $Cu(NO_3)_2$/PVP blended solution was stirred to form a clear, homogeneous and viscous solution for electrospinning.

II) For the electrospinning process, the precursor solution was electrospun for 10 min with a 0.2 mL/h flow rate at 14.5 kV positive voltage. The electrospun nanofibers were collected onto a 1 cm × 4 cm ITO surface on grounded aluminum foil, which were horizontally and perpendicularly placed 25 cm away from the spinneret (see supplementary material Fig. S1). The ambient temperature and relative humidity for electrospinning were around 20 °C and 50%, respectively.

III) The nanofiber-coated ITO was heated at 300 °C for 3 h in the air. During the calcination process, PVP was decomposed and the precursor nanofibers on ITO were transformed to CuO nanofibers. The CuO NFs–ITO film has a sensitive response to glucose and could be directly used as a working electrode to detect glucose. The effective working electrode area immersed in the solution was 1 cm × 1.5 cm, regulated by silastic partly covered on the CuO NFs–ITO film.

2.3. Apparatus

The electrospinning apparatus consisted of a high-voltage power supply (Series EL, Glassman High Voltage Inc.), a syringe pump, a syringe, a stainless steel needle ($d=0.55$ mm) and a grounded collector (ITO fasted on the aluminum foil; see supplementary material Fig. S1). The morphologies of CuO NFs–ITO film were examined using a Hitachi S-4800 ultra-high resolution field emission scanning electron microscope (FESEM; Tokyo, Japan). X-ray diffraction (XRD) measurements were performed on a Tongda TD-3500 X-ray powder diffractometer (Liaoning, China) with Cu Kα radiation ($\lambda=0.154$ nm). The XRD patterns were recorded from 20° to 80° with a scan rate of 0.01°/s. Thermogravimetric analysis (TGA) was performed on a NETZSCH TG 209 F1 under air atmosphere at a flow rate of 50 mL min^{-1}, and the scanning scope was from 40 to 600 °C with a heating rate of 10 °C min^{-1}. The electrochemical measurements of CuO NFs–ITO electrode were performed on an Autolab PGSTAT 12 potentiostat (Amsterdam, The Netherlands). All electrochemical experiments were carried out using a conventional three-electrode system consisting of a saturated calomel reference electrode (SCE), a platinum wire counter electrode and a CuO NFs–ITO working electrode. A 0.15 M NaOH solution was used as the supporting electrolyte.

3. Results and discussion

3.1. Characterization of the CuO nanofibers

X-ray powder diffractometery (XRD) is a reliable technique for investigating the nature of any crystalline material. Fig. 1A shows the XRD patterns of $Cu(NO_3)_2$/PVP nanofibers before and after calcination at 200 °C, 300 °C, 400 °C and 500 °C for 3 h in the air. From the

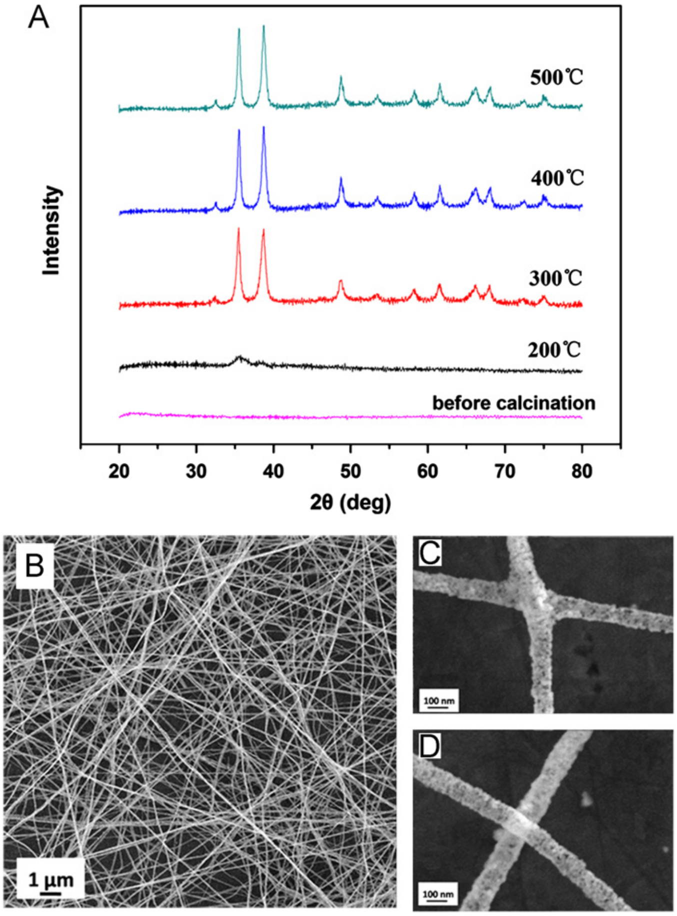

Fig. 1. (A) XRD of Cu$(NO_3)_2$/PVP nanofibers before and after calcination at 200 °C, 300 °C, 400 °C and 500 °C. (B) A typical SEM image of CuO nanofibers on the surface of ITO after calcinated at 300 °C for 3 h in the air. (C) Fused junction between CuO nanofibers. (D) Touched junction between CuO nanofibers.

results, it can be seen that the products after calcination above 300 °C are well crystallized and all of the diffraction peaks could be assigned to the monoclinic structured CuO (JCPDS 05-0661).

The morphologies and microstructures of synthesized CuO nanofibers could be examined by SEM. Fig. 1B presents the typical SEM image of CuO electrospun nanofibers on the surface of ITO. It clearly shows that the CuO nanofibers have been well attached to the surface of ITO after calcination at 300 °C. The fibers are found to be continuous for more than 1 cm with diameters of about 100 nm, resulting in an extremely high aspect ratio. Fig. 1C and D shows two different types of CuO nanofibers conjunction after calcination: fused junction and touched junction, respectively. During the calcination process, with the temperature increasing, the polymer nanofibers became soft and began to decompose, and fused together at contact points (Fig. 1C). Meanwhile, the polymer nanofibers at some distance got close and formed a touched junction (Fig. 1D). Researches have been proved that both the touched junctions and fused junctions could be beneficial for the transport of electrons in materials [37]. From the highly magnified CuO nanofibers, it could be seen clearly that the nanofibers are composed of CuO nanoparticles with a diameters of about 20 nm, which could provide large surface area and high surface energy for catalytic reaction.

3.2. Electrocatalysis of glucose at the CuO NFs–ITO electrodes

The electrocatalytic activity of the CuO NFs–ITO electrodes towards the oxidation of glucose in alkaline medium was demonstrated by cyclic voltammograms (CVs). Fig. 2A displays the CVs of bare ITO and CuO NFs–ITO electrodes in 0.15 M NaOH with the absence (curves a and c) and presence (curves b and d) of 0.10 mM glucose. As shown in Fig. 2A, only a small background current was observed with the bare ITO as working electrode in 0.15 M NaOH (curve a). However, at the same condition, the CuO NFs–ITO electrode exhibited a single broad reduction peak at a potential of 0.52 V (curve c). This may correspond to the Cu(II)/Cu(III) redox couple [38,39]. After the addition of glucose, there

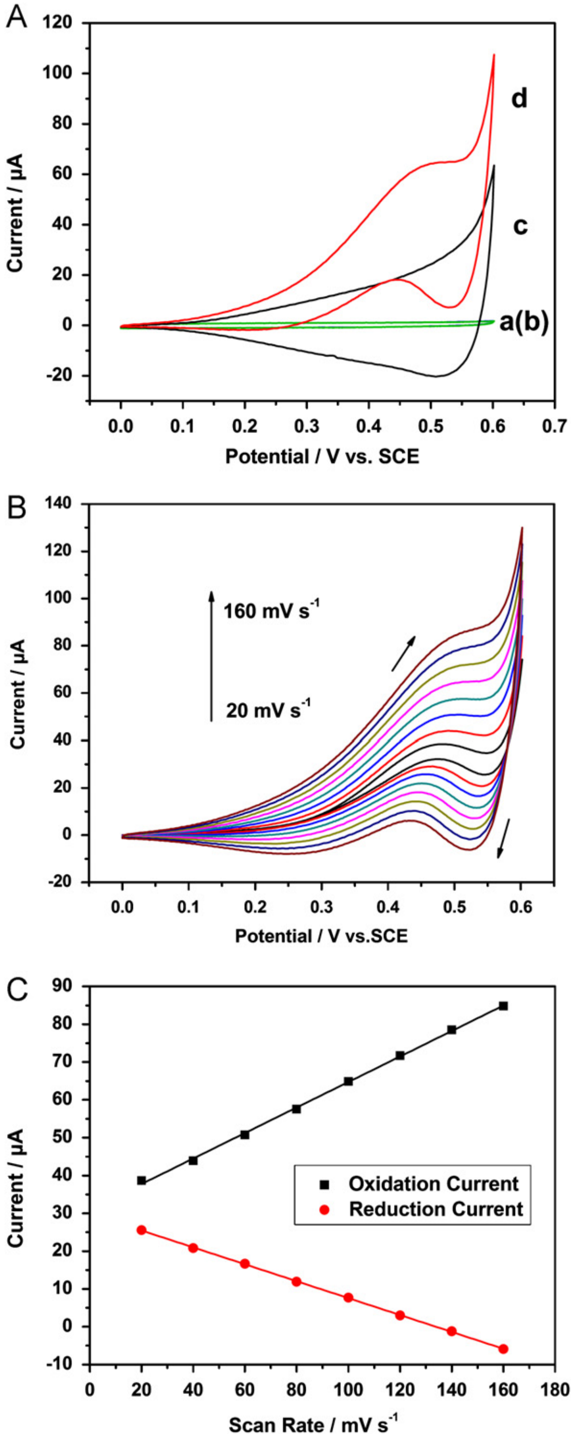

Fig. 2. (A) CVs of ITO (a,b) and CuO NFs–ITO (c and d) in 0.15 M NaOH in the absence (a,c) and presence (b,d) of 0.10 mM glucose, respectively. The scan rate is 100 mV s^{-1}. (B) CVs of CuO NFs–ITO electrode in 0.15 M NaOH in the presence of 0.10 mM glucose at various scan rates: 20, 40, 60, 80, 100, 120, 140, 160 mV s^{-1}. (C) Plot of peak current versus scan rates.

was no response to glucose on bare ITO electrode, suggesting that the direct oxidation of glucose at ITO was not possible (curve b). Comparing with that at ITO, a significant oxidation peak, corresponding to the irreversible glucose oxidation, was observed at CuO NFs–ITO electrode (curve d). The oxidation process starts at approximately 0.30 V vs. SCE, and the current continues to increase until 0.48 V vs. SCE. This may be attributed to the proposed involvement of Cu(II) and Cu(III) surface species in the oxidation of glucose, although the exact mechanism for the oxidation of glucose in alkaline medium at the Cu-based modified electrode is still not clearly known [38,39]. The obvious anodic oxidation peak at 0.48 V shows a strong catalytic function of the CuO nanofibers in the direct oxidation of glucose. The glucose oxidative response at the CuO NFs–ITO electrode is comparable with that of the copper-based electrodes previously reported [16,27,33].

In order to determine the kinetic parameters of glucose oxidation at the CuO NFs–ITO electrode in alkaline medium, the CVs of glucose solution at different scan rates were recorded as depicted in Fig. 2B. The scan rates investigated in this work were from 20 mV s^{-1} to 160 mV s^{-1}. From the results, it could be seen that the redox peak currents are proportional to the scan rates (Fig. 2C), indicating a typical surface controlled electrochemical process with a fast electron-transfer behavior, which is ideal for quantitative analysis in practical applications.

In order to improve its performance, various factors affecting the response of the sensor were investigated, such as the concentration of NaOH, the electrospinning time of nanofibers, the $Cu(NO_3)_2$:PVP mass ratios and the calcination temperature. The effect of each factor on the current response sensitivity of the sensor to glucose was investigated by means of chronoamperometry. The experiments were conducted by exposing the electrode to 50 mL NaOH solution (0.15 M) with each successive addition of 0.10 mM glucose. The detection potential was selected as 0.48 V, according to the oxidation peak on CVs curve (Fig. 2A). When one factor was investigated, other factors were kept consistent with those indicated in the experimental procedure.

Alkaline electrolyte is required for electrooxidation of carbohydrates on Cu as a result of their electrocatalytic effect mediated $Cu(OH)_2$/CuO(OH) redox couples [33]. In order to obtain the optimal measurement conditions for the amperometric sensing of glucose, the effect of NaOH concentration on the response current of the sensor was investigated in this study. The concentrations of NaOH used were 0.0010, 0.010, 0.10, 0.15, 0.20 and 0.50 M, and the results are shown in Fig. 3A. One can see that the CuO NFs–ITO electrode showed no distinguishable current response to glucose in 0.0010 M NaOH solution. With the increase of NaOH concentration, the sensitivity of CuO NFs–ITO electrode to glucose increased until it reached 0.15 M and then the sensitivity of sensor decreased with further increase in NaOH. Therefore, 0.15 M NaOH was chosen as the supporting electrolyte in the following measurements.

The density of CuO nanofibers on ITO, on which the current response sensitivity of CuO NFs–ITO glucose sensor mainly depended, could be controlled by adjusting the electrospinning time. Fig. 4(A,B,C,D and E) shows the SEM of CuO NFs–ITO electrodes, which were spun for 2, 5, 10, 15, 20 min, respectively. From the results, it can be seen that the CuO nanofibers on ITO became denser with the increase of electrospinning time. The optimal electrospinning time was chosen by comparing the sensitivity of CuO NFs–ITO electrodes to glucose. Fig. 4F shows that the sensitivity of the electrode to glucose increases with the electrospinning time until it reaches 10 min, and then decreases with the further increase of electrospinning time. It could be speculated that the increasing amount of CuO nanofibers on ITO could improve the electrocatalytic activity to glucose, however, when the CuO nanofibers film grew thicker, it became easier to be exfoliated from the surface of ITO, which influenced the current response of glucose. Hence, 10 min was chosen as the optimum electospinning time in the electrode manufacturing process.

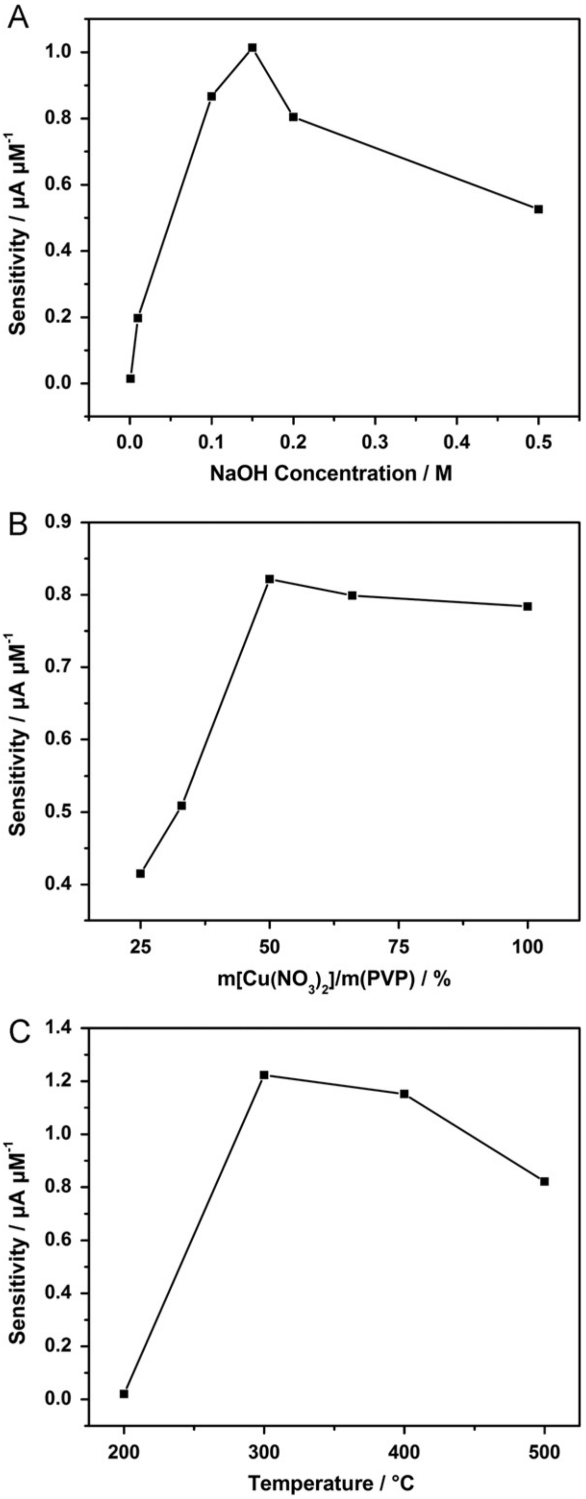

Fig. 3. Effect of NaOH concentration (A), $Cu(NO_3)_2$:PVP mass ratios (B) and calcination temperature (C) on the current response sensitivity of the CuO NFs–ITO electrode to glucose.

The mass ratio of $Cu(NO_3)_2$ to PVP in the precursor solution is one of the important parameters in preparing CuO nanofibers with good morphology and performance. Because the spinnability of the solution is mainly determined by the polymer, the PVP

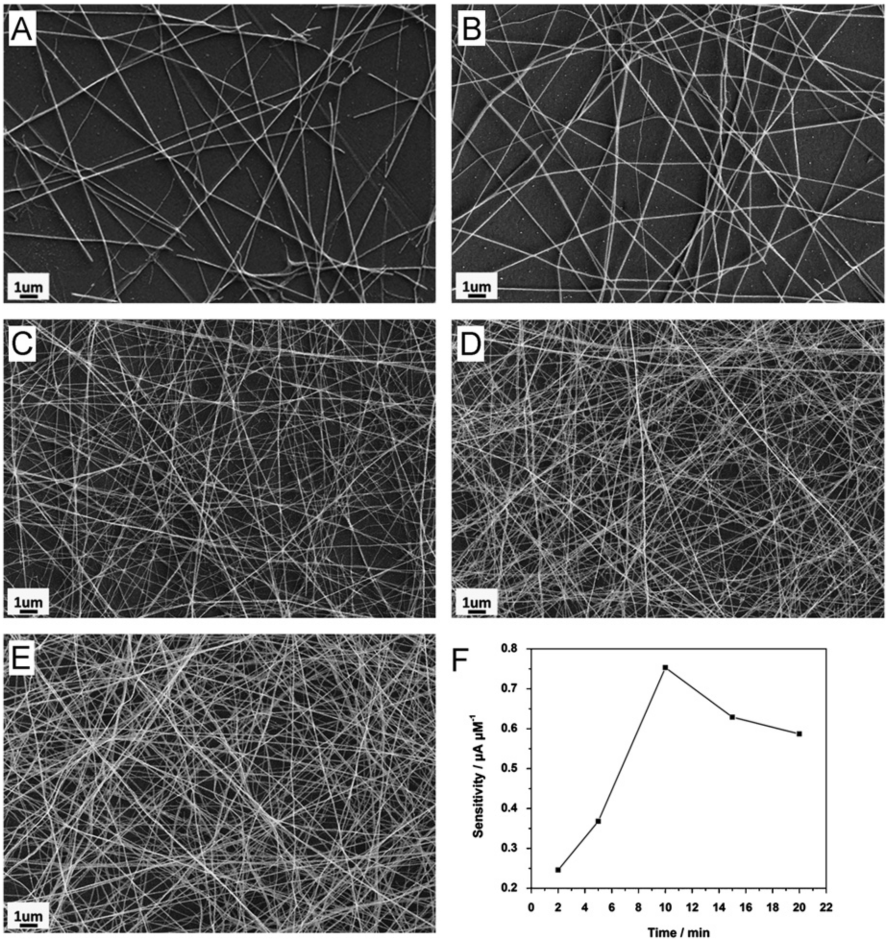

Fig. 4. SEM of CuO NFs–ITO electrodes with different electrospinning times of 2 min (A), 5 min (B), 10 min (C), 15 min (D) and 20 min (E). (F) The current response sensitivity of the CuO NFs–ITO electrode to glucose as a function of electrospinning time.

concentration was maintained constant in this work, and the $Cu(NO_3)_2$ to PVP mass ratios were increased from 25% to 100%. Fig. 3B shows the influence of $Cu(NO_3)_2$:PVP mass ratios on the current response sensitivity of the CuO NFs–ITO electrode to glucose. The maximum sensitivity of the electrode was obtained with a mass ratio of 50%; therefore the $Cu(NO_3)_2$:PVP mass ratio of 50% was chosen in the preparation of precursor solution.

Calcination is a considerable step in the preparation of metal oxide nanofibers. Therefore, the effect of calcination temperature on the sensitivity of CuO NFs–ITO electrodes to glucose was also investigated. The $Cu(NO_3)_2$/PVP NFs-coated ITO were heated at 200 °C, 300 °C, 400 °C and 500 °C for 3 h, and the influence of calcination temperature on the current response sensitivity of CuO NFs–ITO electrode to glucose is shown in Fig. 3C. It can be seen from the results that the electrode, heated at 200 °C, shows no distinguishable response to glucose. The reason is that the $Cu(NO_3)_2$ and PVP could not be decomposed at 200 °C (seen from the thermogravimetric curve of $Cu(NO_3)_2$/PVP composite nanofibers in Supplementary material Fig. S2); when the electrode was put in the solution, the composite nanofibers would be exfoliated from the surface of ITO; then the electrode could be seen as a bare ITO electrode in the solution. The maximum sensitivity of the electrode was obtained at 300 °C, and when the calcination temperature increased from 300 °C to 500 °C, the response to glucose decreased significantly. In order to find out the reason for this phenomenon, the electrochemical impedance spectra (EIS) of the CuO NFs–ITO electrodes calcinated at different temperatures were acquired and the corresponding Nyquist plots are presented in Fig. 5. The EIS pattern shows a semicircular part at high frequency attributed to the charge transfer impedance (R_{ct}) and a linear part of the Warburg impedance (Z_w) in the low frequency range, which could be well simulated by the Randle's equivalent circuit (inset of Fig. 5 and Supplementary material Table S1)[40]. The R_{ct} of the CuO NFs–ITO electrodes heated at 300, 400 and

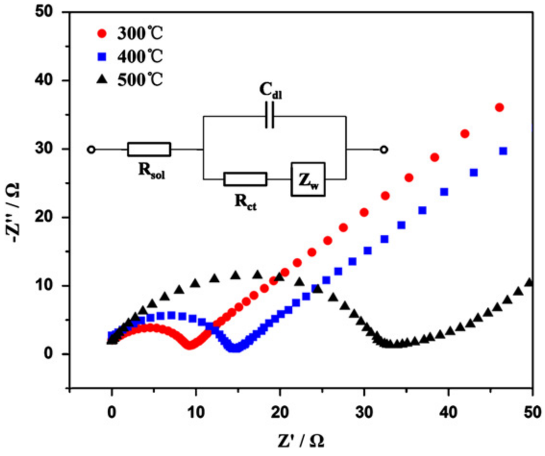

Fig. 5. Nyquist plots of CuO NFs–ITO electrodes prepared at different calcination temperatures. The frequency range is from 0.01 Hz to 100 kHz, and the amplitude is 0.010 V. All electrodes are tested in 5.0 mM Fe(CN)$_6^{3-/4-}$ and 0.10 M KCl solution at open circuit potential. Inset displays the Randles equivalent circuit.

500 °C were 8.48, 14.13 and 32.70 Ω, respectively. Obviously, the R_{ct} increased with the increase of the calcination temperature, indicating that better current response sensitivity could be obtained at lower temperature. Therefore, 300 °C was chosen as the calcination temperature for the following measurements.

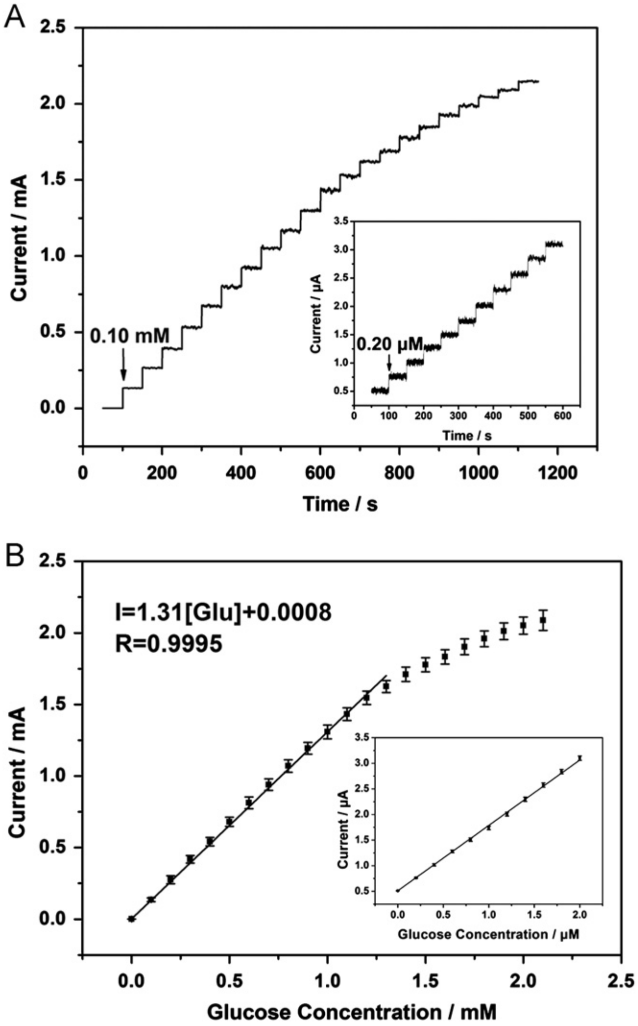

Fig. 6. (A) Amperometric response of CuO NFs–ITO electrode with successive additions of 0.10 mM glucose to 0.15 M NaOH at 0.48 V. The inset shows amperometric response with successive additions of 0.20 μM glucose. (B) The typical calibration curve of current vs. glucose concentration. The inset displays the calibration curve in the concentration range of 0.20 μM to 2.0 μM.

3.3. Amperometric analysis

Under the optimized experimental conditions, the performance of the CuO NFs–ITO glucose sensor was investigated by amperometric analysis. Fig. 6A displays a typical amperometric response curve of CuO NFs–ITO electrode with successive injections of 0.10 mM glucose to 0.15 M NaOH at 0.48 V, and the inset of Fig. 6A shows amperometric responses under successive additions of low concentration of glucose (0.20 μM). The results show that with the successive additions of glucose into 0.15 M NaOH, a stable and fast amperometric response could be observed at 0.48 V. The response time, which reached the steady state after the addition of glucose, was less than 1 s, indicating a rapid oxidative process of glucose on the surface of CuO NFs–ITO electrode. The calibration curve for the glucose sensor is shown in Fig. 6B, and the inset of Fig. 6B shows the calibration curve in the concentration range of 0.20–2.0 μM. The plots reveal that the sensor has a good linear response to glucose ranging from 0.20 μM to 1.3 mM with a correlation coefficient of 0.9995, a sensitivity of 1.31 mA mM^{-1} (873 μA mM^{-1} cm^{-2}), and a detection limit of 40 nM with a signal/noise ratio of 3. The parameters of our CuO nanofibers modified ITO electrode, such as the sensitivity, the linear range and the detection limit, are compared with those of other CuO nanomaterials or electrospun nanomaterials modified nonenzymatic glucose sensors [16,17,25,27,32–34]. As listed in Table 1, the sensitivity, the detection limit and the linear range of our present nonenzymatic glucose sensor are comparable and even better than those of other sensors. The high sensitivity, low detection limit and fast response time of the CuO NFs–ITO glucose sensor should be attributed to the directly prepared CuO nanofibers on ITO. Firstly, the $Cu(NO_3)_2$/PVP nanofibers were directly spun onto the surface of ITO, and then used as a working electrode to determine glucose after the calcination in this study. This CuO NFs–ITO electrode preparation method ensures the direct electron transfer between the CuO nanofibers and the ITO electrode, and thus enhances the sensitivity of sensor to glucose. In addition, the touched junctions and fused junctions between CuO nanofibers (see Fig. 1) could also promote the electron transfer rate in the process of glucose oxidation. Therefore, the CuO NFs–ITO electrode prepared in this study can greatly increase the electrocatalytic active areas and promote electron transfer in the electro-oxidation of glucose, and then enhance the sensitivity of the nonenzymatic glucose sensor.

The reproducibility, stability and selectivity of the sensor were evaluated. The current responses of five CuO NFs–ITO electrodes to 0.10 mM glucose at 0.48 V were investigated, and the relative standard deviation (RSD) of 3.3% was obtained, indicating a high reproducibility of this procedure. The electrode could be cleaned with voltammetric cycles from 0 to 0.60 V for 20 cycles in 0.15 M NaOH to eliminate the adsorption after each determination; nine

Table 1
Comparison of analytical performance of our proposed CuO NFs–ITO electrode with those of other nonenzymatic glucose sensors.

Electrode	Sensitivity	Detection limit	Linear range	Reference
CuO NFs/ITO electrode	873 μA mM^{-1} cm^{-2}	40 nM	0.20 μM–1.3 mM	This work
CuO NFs/glass carbon electrode	431 μA mM^{-1} cm^{-2}	0.8 μM	6.0 μM–2.5 mM	[33]
CuO nanowires/Cu electrode	490 μA mM^{-1}	50 nM	0.40 μM–2.0 mM	[16]
CuO nanorods/graphite electrode	371 μA mM^{-1} cm^{-2}	4 μM	4.0 μM–8.0 mM	[27]
CuO flowers/graphite electrode	710 μA mM^{-1} cm^{-2}	4 μM	–	[27]
CuO nanospheres/glass carbon electrode	404 μA mM^{-1} cm^{-2}	1 μM	Up to 2.6 mM	[25]
Co_3O_4 NFs–nafion/glass carbon electrode	36.2 μA mM^{-1} cm^{-2}	1 μM	Up to 2.0 mM	[17]
NiO microfibers/fluorine tin oxide electrode	1780 μA mM^{-1} cm^{-2}	30 nM	1 μM–0.27 mM	[34]
Ni nanoparticle-loaded C NFs electrode	420 μA mM^{-1} cm^{-2}	1 μM	2 μM–2.5 mM	[32]

successive measurements of 0.10 mM glucose on one CuO NFs–ITO electrode yielded an RSD of 1.6%, confirming that the modified electrode had excellent ability to prevent the electrode from fouling by the oxidation product. In addition, the stability of CuO NFs–ITO electrode was also evaluated by measuring its current response to 0.10 mM glucose within a 30-day period (Supplementary material Fig. S3). The sensor was stored in air at ambient conditions and its current response was tested every 3–10 days. The results demonstrated that the current response signal to glucose retained 92% of its original activity after being stored for 1 month, demonstrating a long-term storage stability of the electrode. The high reproducibility and stability of CuO NFs–ITO sensor are desirable for most routine analysis.

For a sensor, the selectivity is very important, especially for the real sample testing. It has been reported that the electrochemical glucose sensors based on Cu electrodes could easily lose their activity due to the chloride poisoning effect [16]. Thus the test was examined by adding sodium chloride in the supporting electrolyte in measurement. In addition, there are lots of co-existing electroactive species which might affect the sensor's response, such as ascorbic acid (AA), uric acid (UA), dopamine (DA), sucrose, lactose and soluble starch. Among those, some easily oxidizable species, such as ascorbic acid (AA) and uric acid (UA), could greatly affect glucose test results. The normal physiological level of glucose is about 3–8 mM and the interfering species such as AA and UA are about 0.1 mM [16]. Therefore, the effect of these potential interferents on the response of the CuO NFs non-enzymatic glucose sensor was evaluated. In this work, interference tests were carried out by adding 0.10 mM glucose with additions of 200 mM NaCl, 0.010 mM sucrose, 0.010 mM lactose, 0.010 mM soluble starch, 0.010 mM AA, 0.010 mM UA, and 0.010 mM DA in 0.15 M NaOH. As shown in Fig. 7, all the potential interferences tested in this work caused almost negligible response, and the results are summarized in the bottom table of Fig. 7. The glucose sensor showed no observable response to 200 mM NaCl, demonstrating that the electrode can be used in the presence of high concentration chloride ions. In summary, our results demonstrate that the CuO NFs/ITO electrode shows high selectivity for glucose detection.

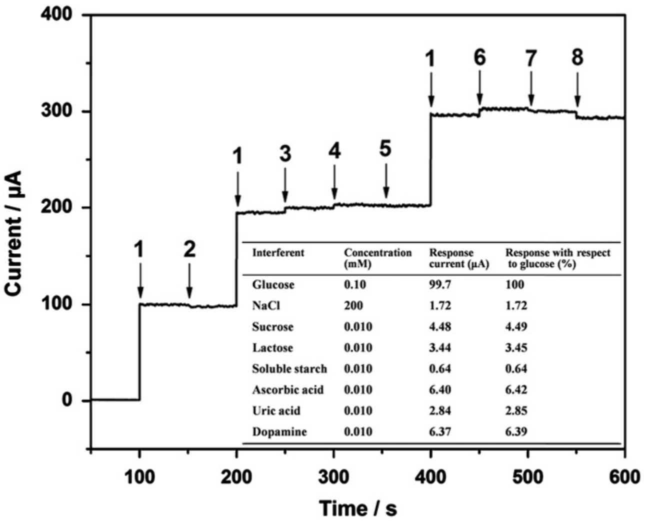

Interferent	Concentration (mM)	Response current (μA)	Response with respect to glucose (%)
Glucose	0.10	99.7	100
NaCl	200	1.72	1.72
Sucrose	0.010	4.48	4.49
Lactose	0.010	3.44	3.45
Soluble starch	0.010	0.64	0.64
Ascorbic acid	0.010	6.40	6.42
Uric acid	0.010	2.84	2.85
Dopamine	0.010	6.37	6.39

Fig. 7. Effect of interferents on the amperometric response of the CuO NFs–ITO electrode: (1) 0.10 mM glucose, (2) 200 mM NaCl, (3) 0.010 mM sucrose, (4) 0.010 mM lactose, (5) 0.010 mM soluble starch, (6) 0.010 mM AA, (7) 0.010 mM UA, and (8) 0.010 mM DA in 0.15 M NaOH at 0.48 V. The bottom table displays the response result of the CuO NFs–ITO electrode to the interferents.

Finally, to illustrate the feasibility of the glucose biosensor in practical analysis, the CuO NFs–ITO electrode was employed to measure the glucose content in some commercial glucose injections. Different standard glucose injection solutions were measured at 0.48 V in 0.15 M NaOH. In addition, the recovery test was conducted. All the data are summarized in Table 2. This table shows that the results obtained by the proposed sensor are satisfactory and agree closely with their real values, revealing the excellent and accurate measurement for glucose determination.

4. Conclusion

In this work, CuO nanofibers were in situ formed onto ITO surface through calcination after the electrospinning. The CuO NFs/ITO electrode had a fast current response to glucose and could be used for the fabrication of nonenzymatic glucose sensor. The direct electron transfer between CuO nanofibers and ITO electrode can effectively improve electrochemical and electrocatalytic performances for glucose sensing. The touched junctions and fused junctions between CuO nanofibers can also increase the electrocatalytic active areas and promote electron transfer in the oxidation of glucose. The effect of NaOH concentration, electrospinning time, $Cu(NO_3)_2$:PVP mass ratios, and calcination temperature on the current response sensitivity for glucose were investigated in detail. Under the optimized conditions, CuO NFs–ITO electrode showed high sensitivity (873 $\mu A\ mM^{-1}\ cm^{-2}$) and low detection limit (40 nM at $S/N=3$) to glucose. In addition, the prepared electrode also offered good reproducibility, stability and selectivity for the glucose detection. The CuO NFs–ITO electrode is easily, inexpensive fabricated and can be used as an amperometric sensor for routine analysis of glucose in some commercial products.

Table 2
Determination and recovery of glucose in *glucose injections* using the proposed CuO NFs-ITO glucose sensor.

Sample[a]	Claimed glucose concentration (g/100 mL)	Concentration of glucose[b] (g/100 mL)	RSD[c] (%)	Glucose added (mM)	Glucose founded (mM)	Recovery (%)	RSD[c](%)
1	5	5.05	2.32	1.00	1.02	102	0.98
2	10	9.90	2.67	1.00	1.03	103	1.69
3	50	50.4	1.43	2.50	2.52	101	1.88
4	50	49.2	3.26	2.50	2.46	98.4	2.24
5	50	50.6	2.76	2.50	2.56	102	2.34

[a] Samples of glucose injection were obtained from different companies.
[b] Determined by this work.
[c] Three replicates were performed.

Acknowledgments

We would express our sincere thanks to the financial support from the National Natural Science Foundation of China (Grant no. 20927007, 21175094) and Youth Foundation of Sichuan University (Grant no. 2010SCU11048) is gratefully acknowledged. Guangyue Liu and Baozhan Zheng contributed equally to this work.

Appendix A. Supporting information

Supplementary data associated with this article can be found in the online version at http://dx.doi.org/10.1016/j.talanta.2012.08.040.

References

[1] C. Deng, Y. Peng, L. Su, Y.N. Liu, F. Zhou, Anal. Chim. Acta 719 (2012) 52–56.
[2] K.J. Cash, H.A. Clark, Trends Mol. Med. 16 (2010) 584–593.
[3] O. Courjean, N. Mano, J. Biotechnol. 151 (2011) 122–129.
[4] B. Zheng, S. Xie, L. Qian, H. Yuan, D. Xiao, M.M.F. Choi, Sensors Actuators B: Chem. 152 (2011) 49–55.
[5] H. Tang, F. Yan, Q. Tai, H.L.W. Chan, Biosensors Bioelectron. 25 (2010) 1646–1651.
[6] M. Ahmad, C. Pan, Z. Luo, J. Zhu, J. Phys. Chem. C 114 (2010) 9308–9313.
[7] B. Zheng, L. Qian, H. Yuan, D. Xiao, X. Yang, M.C. Paau, M.M.F. Choi, Talanta 82 (2010) 177–183.
[8] H. Nie, Z. Yao, X. Zhou, Z. Yang, S. Huang, Biosensors Bioelectron. 30 (2011) 28–34.
[9] S. Hrapovic, Y. Liu, K.B. Male, J.H.T. Luong, Anal. Chem. 76 (2003) 1083–1088.
[10] L. Meng, J. Jin, G. Yang, T. Lu, H. Zhang, C. Cai, Anal. Chem. 81 (2009) 7271–7280.
[11] Y. Li, Y.Y. Song, C. Yang, X.H. Xia, Electrochem. Commun. 9 (2007) 981–988.
[12] J. Yang, W.D. Zhang, S. Gunasekaran, Biosensors Bioelectron. 26 (2010) 279–284.
[13] J.H. Shim, A. Cha, Y. Lee, C. Lee, Electroanalysis 23 (2011) 2057–2062.
[14] J. Wang, D.F. Thomas, A. Chen, Anal. Chem. 80 (2008) 997–1004.
[15] J. Ryu, K. Kim, H.S. Kim, H.T. Hahn, D. Lashmore, Biosensors Bioelectron. 26 (2010) 602–607.
[16] Z. Zhuang, X. Su, H. Yuan, Q. Sun, D. Xiao, M.M.F. Choi, Analyst 133 (2008) 126–132.
[17] Y. Ding, Y. Wang, L. Su, M. Bellagamba, H. Zhang, Y. Lei, Biosensors Bioelectron. 26 (2010) 542–548.
[18] X.J. Zhang, A.X. Gu, G.F. Wang, Y. Huang, H.Q. Ji, B. Fang, Analyst 136 (2011) 5175–5180.
[19] M.U. Anu Prathap, B. Kaur, R. Srivastava, J. Colloid Interface Sci. 370 (2012) 144–154.
[20] S.W. Yun, J.H. Koh, J. Phys. Chem. Solids 73 (2012) 568–572.
[21] R. Sahay, J. Sundaramurthy, P. Suresh Kumar, V. Thavasi, S.G. Mhaisalkar, S. Ramakrishna, J. Solid State Chem. 186 (2012) 261–267.
[22] A. El-Trass, H. ElShamy, I. El-Mehasseb, M. El-Kemary, Appl. Surf. Sci. 258 (2012) 2997–3001.
[23] H. Jin-Woo, M. Meyyappan, Appl. Phys. Lett. 98 (2011).
[24] T. Ghodselahi, H. Zahrabi, M.H. Saani, M.A. Vesaghi, J. Phys. Chem. C 115 (2011) 22126–22130.
[25] E. Reitz, W. Jia, M. Gentile, Y. Wang, Y. Lei, Electroanalysis 20 (2008) 2482–2486.
[26] X. Zhang, G. Wang, X. Liu, J. Wu, M. Li, J. Gu, H. Liu, B. Fang, J. Phys. Chem. C 112 (2008) 16845–16849.
[27] X. Wang, C. Hu, H. Liu, G. Du, X. He, Y. Xi, Sensors Actuators B: Chem. 144 (2010) 220–225.
[28] Z.M. Huang, Y.Z. Zhang, M. Kotaki, S. Ramakrishna, Compos. Sci. Technol. 63 (2003) 2223–2253.
[29] D. Li, Y.N. Xia, Adv. Mater. 16 (2004) 1151–1170.
[30] B. Ding, M. Wang, J. Yu, G. Sun, Sensors 9 (2009) 1609–1624.
[31] B. Ding, M. Wang, X. Wang, J. Yu, G. Sun, Mater. Today 13 (2010) 16–27.
[32] Y. Liu, H. Teng, H. Hou, T. You, Biosensors Bioelectron. 24 (2009) 3329–3334.
[33] W. Wang, L. Zhang, S. Tong, X. Li, W. Song, Biosensors Bioelectron. 25 (2009) 708–714.
[34] F. Cao, S. Guo, H. Ma, D. Shan, S. Yang, J. Gong, Biosensors Bioelectron. 26 (2011) 2756–2760.
[35] D. Li, Y. Xia, Nano Lett. 3 (2003) 555–560.
[36] D. Li, J.T. McCann, Y. Xia, M. Marquez, J. Am. Ceram. Soc. 89 (2006) 1861–1869.
[37] H. Wu, L. Hu, M.W. Rowell, D. Kong, J.J. Cha, J.R. McDonough, J. Zhu, Y. Yang, M.D. McGehee, Y. Cui, Nano Lett. 10 (2010) 4242–4248.
[38] S.T. Farrell, C.B. Breslin, Electrochim. Acta 49 (2004) 4497–4503.
[39] L.D. Burke, G.M. Bruton, J.A. Collins, Electrochim. Acta 44 (1998) 1467–1479.
[40] L.P. Lu, S.Q. Wang, X.Q. Lin, Anal. Chim. Acta 519 (2004) 161–166.